International Journal of Remote Sensing
Vol. 27, No. 21, 10 November 2006, 4847–4866

Taylor & Francis
Taylor & Francis Group

Inundated wetland dynamics over boreal regions from remote sensing: the use of Topex-Poseidon dual-frequency radar altimeter observations

F. PAPA*†‡§, C. PRIGENT†, W. B. ROSSOW§, B. LEGRESY‡ and F. REMY‡
†Laboratoire d'Etude du Rayonnement et de la Matière en Astrophysique, Observatoire de Paris, 61, av. de l'Observatoire, 75014 Paris, France
‡Laboratoire d'Etudes en Géodésie et Océanographie Spatiales, Centre National d'Etudes Spatiales, 18, av. E. Belin 31400 Toulouse, France
§NASA-Goddard Institute for Space Studies, 2880 Broadway, New York, NY, 10025, USA

(*Received 15 March 2005; in final form 5 March 2006*)

This study presents a first attempt to estimate the extent and seasonality of northern wetlands using radar altimeter satellite observations. The sensitivity of the Topex-Poseidon dual-frequency radar altimeter to detect inundation is investigated and compared with passive and active microwave satellite measurements along with a land surface climatology database. The C band backscatter altimeter signal clearly tracks passive microwave emissivity observations of wetlands and is able to detect small flooded areas. Because of the nadir incidence angle, the radar altimeter also shows more capability to detect wetlands than the C band scatterometer. Monthly flooded areas are calculated by estimating flooded pixel fractional coverage using the altimeter C band backscatter magnitude and a linear mixing model with dual-frequency altimeter backscatter difference, C–Ku, to account for vegetation effects. Because of the Topex-Poseidon satellite spatial coverage, the results are given only from 40° N to 66° N. This region nevertheless represents more than 30% of world's inundated surfaces during the summer. A direct validation of the inundated extent is unfortunately impossible on a large scale, due to the scarcity of quantitative observations. As a consequence, the results are evaluated by comparison with other existing estimates. Radar altimetry estimates, comprising natural wetlands and river/lakes, indicate a maximum inundated area of $1.86 \times 10^6\,km^2$ for July 1993 and 1994 as compared with $1.31 \times 10^6\,km^2$ from passive microwave technique and $\sim 2.10 \times 10^6\,km^2$ from climatology dataset. The wetland seasonal variability derived from the altimeter and passive microwave techniques agrees well. These promising results could soon be applied to the ENVISAT dual-frequency radar altimeter that will provide a better survey of global inundated surfaces thanks to its much more complete spatial coverage.

1. Introduction

Wetlands are the world's largest methane source (CH_4) and the only source dominated by climate variations. Although not exceeding ~4% of the Earth's ice-free land surface, inundated wetlands account for ~40% of CH_4 emissions annually in the atmosphere. Wetlands are also the major source influencing interannual

*Corresponding author. Email: fpapa@ giss.nasa.gov

International Journal of Remote Sensing
ISSN 0143-1161 print/ISSN 1366-5901 online
http://www.tandf.co.uk/journals
DOI: 10.1080/01431160600675887

variations in atmospheric growth rate of methane (Matthews 2000), especially considering that ~60% of wetlands are only inundated for some portion of the year. About 30% of total methane emission comes from northern wetlands (Walter *et al.* 2001), representing one of the most important contributions to methane large interannual variability growth (Walter *et al.* 2001). In addition, boreal wetlands play a key role for local hydrological system during the summer period (Allison and Goodison 2001). The part of the fresh water input in the northern oceans by river discharge is crucial to determine as it greatly influences the ocean circulation and winter sea ice cover (Dickinson *et al.* 2001). Since uncertainties of their seasonal and inter-annual extents are large, high northern latitude inundated surfaces are crucial to measure more systematically.

Monitoring boreal wetland dynamics and their climate-sensitive processes is crucial in better understanding their influence on future climate through their role in the global carbon cycle, as well as their role in the prediction of inter-annual and longer-term climate variations.

Despite the difficulties in monitoring wetlands and their dynamics at large scale, global wetlands have been investigated using different techniques with varying degrees of success. The first datasets representing realistic global wetland distributions were based on compilations of *in situ* soil and vegetation observations (Matthews and Fung 1987, Cogley 1991), but unfortunately they suffer from a lack of information on temporal and spatial dynamics. Satellite observations provide a means of monitoring wetlands and their dynamics at global and regional scales over long time periods. Recently, remote sensing techniques and space-borne sensor observations in different parts of the electromagnetic spectrum have been explored to characterize wetland inundation and their variations. Visible or infrared observations (for instance from the Advanced Very High Resolution Radiometer) provide high spatial resolution but are limited by their inability to penetrate clouds or vegetation. Use of passive microwave observations (e.g. from the Scanning Multi-Channel Microwave Radiometer (SMMR) or from the Special Sensor Microwave/Imager (SSM/I)) illustrates their capability to detect inundated areas (Sippel *et al.* 1998). However, over vegetated wetlands there are difficulties in accounting for vegetation attenuation when using only passive microwave observations (Justice *et al.* 1989). A promising technique considering a suite of complementary satellite observations was developed to quantify spatial and temporal dynamics of wetlands (Prigent *et al.* 2001a). It is based on the detection of inundations at the global scale using the passive microwave land-surfaces emissivities estimated from SSM/I observations, and the use of ERS scatterometer and AVHRR visible and near infrared reflectances to estimate the vegetation contribution to the passive microwave signal (Prigent *et al.* 2001b).

Satellite-altimeter radars are active microwave sensors initially launched to operate over the ocean (Fung and Cazenave 2001). However, this technique soon exhibited potential for the study of continental surfaces (Zwally *et al.* 1983), especially to estimate accurately the topography of ice-covered regions such as Antarctica or Greenland (Legresy and Remy 1997, Rémy *et al.* 1999) or to monitor large continental water surfaces and measure their stage elevation for hydrological applications (Birkett 1995, Cazenave *et al.* 1997, Alsdorf *et al.* 2001). Recently, the altimeter response was investigated over land surfaces using dual-frequency backscattering coefficients from the French-American Topex-Poseidon satellite or the new ESA ENVISAT satellite (Papa *et al.* 2003, Kouraev *et al.* 2003, Legresy *et al.*

2005). New capabilities of the radar altimeters were demonstrated to characterize and monitor vegetated areas, deserts, semi-arid and boreal regions at global scale. The Topex-Poseidon altimeter was also successfully used to retrieve snow depth evolution over the Northern Great Plains (Papa *et al*. 2002).

The objective of the present study is to compare the altimetric response to the other microwave observations (passive and active) over inundated regions and to demonstrate the capability of radar altimetry to monitor the spatial and seasonal dynamics of the wetlands. So far, hydrological studies using inland altimetry have been developed for regional studies (Birkett 1998, 2000, Alsdorf *et al*. 2001) and only the single Ku band frequency measurements have been explored for this purpose. We propose to analyse the altimetric observations from the CNES/NASA Topex-Poseidon (T-P) launched in August 1992. The NASA Radar Altimeter (NRA) on board this satellite is the first dual-frequency active microwave sensor, with nadir measurements at Ku (13.6 GHz) and C (5.4 GHz) bands. This study will focus on northern wetlands in the boreal regions above 40° N where Topex-Poseidon provides adequate spatial coverage.

The data are presented in §2, and §3 compares the responses of satellite microwave sensors, passive and active, over the northern latitudes during 1993–1994, with a special focus on the Ob region. In §4 the new methodology is presented, as well as the results obtained using the Topex-Poseidon dual-frequency radar altimeter to detect wetlands and to quantify their dynamics. For the Ob region, the seasonal cycle of inundated extent is compared to T-P radar altimeter measurements of the river level dynamics (Kouraev *et al*. 2004). As no validation data exist at such large scales, the results are also evaluated by comparison with existing climatological datasets.

2. Datasets

2.1 *The Topex-Poseidon satellite*

Topex-Poseidon is the first satellite of a joint US and French radar altimeter mission initially developed to make accurate measurements of sea level (Zieger *et al*. 1991). From its launch in August 1992 to present, Topex-Poseidon observes the ocean and continental surfaces along its orbit ground track from 66° N to 66° S with a 10-day repeat cycle (the satellite passes over the same point every 9.91 days). The T-P equatorial ground spacing is about 300 km and its swath width only amounts to a few kilometers.

In this study, we only use observations from the principal instrument onboard Topex-Poseidon satellite, the NRA (NASA Radar Altimeter), a dual-frequency radar altimeter operating in K_u band (frequency 13.6 GHz, wavelength 2.3 cm) and C band (frequency 5.4 GHz frequency, wavelength 5.8 cm); the dual frequency was initially designed to provide corrections on the height measurement errors due to the ionospheric delays on the microwave signal. Rodriguez and Martin (1994) present details of the characteristics and the performance of the T-P altimeter.

Four parameters can be obtained from the altimeter waveform retracking technique (Legresy and Remy 1997, Legresy *et al*. 2005): the altimetric height, the backscattering coefficient, the leading edge width and the slope of the trailing edge. In this study, we only analyse the backscattering coefficients in C and Ku bands expressed in decibels (dB). A precise description of dual-frequency radar altimeter backscatter from T-P over continental surfaces and inland water surfaces can be found in Papa *et al*. (2003).

With its inter-track spacing about ~300 km, Topex-Poseidon spatial coverage is too sparse to study the wetlands characteristics globally, especially considering the low latitudes regions. As a consequence, the present study is focused on northern wetlands of the boreal regions. At such latitudes (>50° N), the T-P spatial coverage is much more adequate with an inter-track spacing reduced. Over a month, for the highest latitudes, at least 10 values on average are obtained in a cell.

Considering the precision of the measurements, note that for the T-P altimeter, the backscattering coefficient is measured every second (representing 7 km intervals along the satellite track) and its precision is better than 1 dB for the highest latitudes (>50° N), so that the average precision at this scale is approximately 0.26 dB (Papa *et al.* 2003)

2.2 *The other microwave satellite observations*

In this study, the altimetric observations are compared to other available microwave satellite measurements that have already been used for wetland characterization. The objective is to evaluate and compare the sensitivity of these observations to the presence of open water at the surface in order to understand better the observations and to benefit from their complementarities.

1. **Passive microwave measurements at 19 and 37 GHz from SSM/I**. The Special Sensor Microwave/Imager (SSM/I) onboard the Defense Meteorological Satellite Program (DMSP) observes the Earth twice daily at 19.35, 22.235, 37.0 and 85.5 GHz with both vertical and horizontal polarizations, except for the 22 GHz channel, which is vertical polarization only (Hollinger *et al.* 1990). The observing incidence angle is close to 53° and the elliptical fields of view decrease in size proportionally with frequency, from 43×69 to $13 \times 15\,km^2$. In this study, we use the microwave SSM/I emissivities at 19 GHz and 37 GHz, horizontally and vertically polarized, estimated from the SSM/I brightness temperatures when combined with infrared brightness temperatures, removing the atmosphere, cloud, and rain contributions (Prigent *et al.* 1997).
2. **Active microwave observations from the ERS-1 scatterometer at 5.25 GHz**. In 1991, the European Space Agency (ESA) launched its first multi-sensor satellite devoted to Earth observation ERS. On board, the ERS wind-scatterometer is primarily devoted to ocean observation but early on showed potential for continental studies (Frison and Mougin 1996a, Prigent *et al.* 2001b). It operates at C band (5.25 GHz) vertical polarization with a 50 km spatial resolution and continuously measures a backscattering coefficient (dB) with three antennas scanning the land surfaces in three different azimuthal directions with viewing angles ranging from 18° to 59°. With the scatterometer operating continuously, global coverage is achieved in four days. The scatterometer response is very stable over time for non-changing targets and the uncertainties are estimated to be about 5%. Water vapour and cloud absorption/emission are negligible at 5.25 GHz and no atmospheric correction is required. Backscattering coefficients data used in this study are processed in accordance with the Frison and Mougin (1996b) method, considering a linear fit calculated for all incidence angles between 25° and 50° for a month and keeping the fitted value at 45°

A more detailed description of the SSM/I and ERS products used in this study can be found in Prigent *et al.* (2001b).

The satellite data used in this study are monthly averages mapped into an equal-area grid of 0.25° resolution at the equator, compatible with the different satellite resolutions. Two years of satellite observations have been examined (January 1993 to December 1994). Only measurements over continents are considered, and coastal observations have been excluded to avoid contamination with signal coming from the ocean.

2.3 *Land surface databases and wetland estimates with a suite of satellites*

Independent land surface databases are used to help assess the sensitivity of the satellite observations to the land characteristics, essentially the presence of water and vegetation.

Matthews and Fung (1987) give the wetland fractions for each $1^\circ \times 1^\circ$ over the globe, obtained from aeronautical charts during the warm season, which usually corresponds to maximum flooding. The Cogley (1991) dataset represents a worldwide distribution of wetlands and small lakes with a $1^\circ \times 1^\circ$ spatial resolution. Matthews (1983) vegetation and land use datasets were compiled from a large number of published sources and distinguish at a $1^\circ \times 1^\circ$ spatial resolution a large number of vegetation types, typically grouped in 10–30 classes of natural vegetation. For the study, we regridded these land surface data on the same equal-area resolution of 0.25° at the equator.

In this study, we also use as an independent dataset of comparison with the altimeter results, the methodology developed in Prigent *et al.* (2001a), which quantifies the extent and seasonality of inundation on the global scale using a suite of satellites. The selected satellite observations used to detect wetlands in this method cover a large wavelength range: (a) passive microwave SSM/I emissivities at 37 GHz (0.81 cm); (b) ERS-1 active microwave scatterometer backscatter at 5.25 GHz (5.71 cm); and (c) AVHRR Normalized Difference Index Vegetation NDVI. As a first step, all remote sensing data are monthly averaged in an equal area resolution of 0.25° at the equator for the period 1993–1994 available at this time. The proposed methodology to estimate monthly flooded areas is then based on the estimation of pixel fractional coverage by open water using the passive microwave signal and a linear mixture model with end-members calibrated with radar observations to account for the effects of vegetation cover (Prigent *et al.* 2001a).

3. Analysis of the altimetric response over boreal wetlands and comparison with other microwave satellite observations

3.1 *Altimetric observations over the boreal region*

Figure 1 illustrates the geographic patterns found in the Topex-Poseidon backscatter in the C band (a) and the difference in backscatter C–K_u (b), expressed in decibels (dB), for the latitudes from 40° N to 66° N for July 1993. The altimeter backscatter results from two contributions, a surface echo and a volume echo (Papa *et al.* 2003), which are related to the land surface characteristics. Over the considered regions, a large spatial dynamic range of more than 35 dB is observed in C band. For the difference C–K_u, the variation is more than 10 dB. Different climate-related factors have an impact on the measured altimeter backscatter in C and Ku bands. However, precipitation (one of these main factors) only effects the backscatter measurements

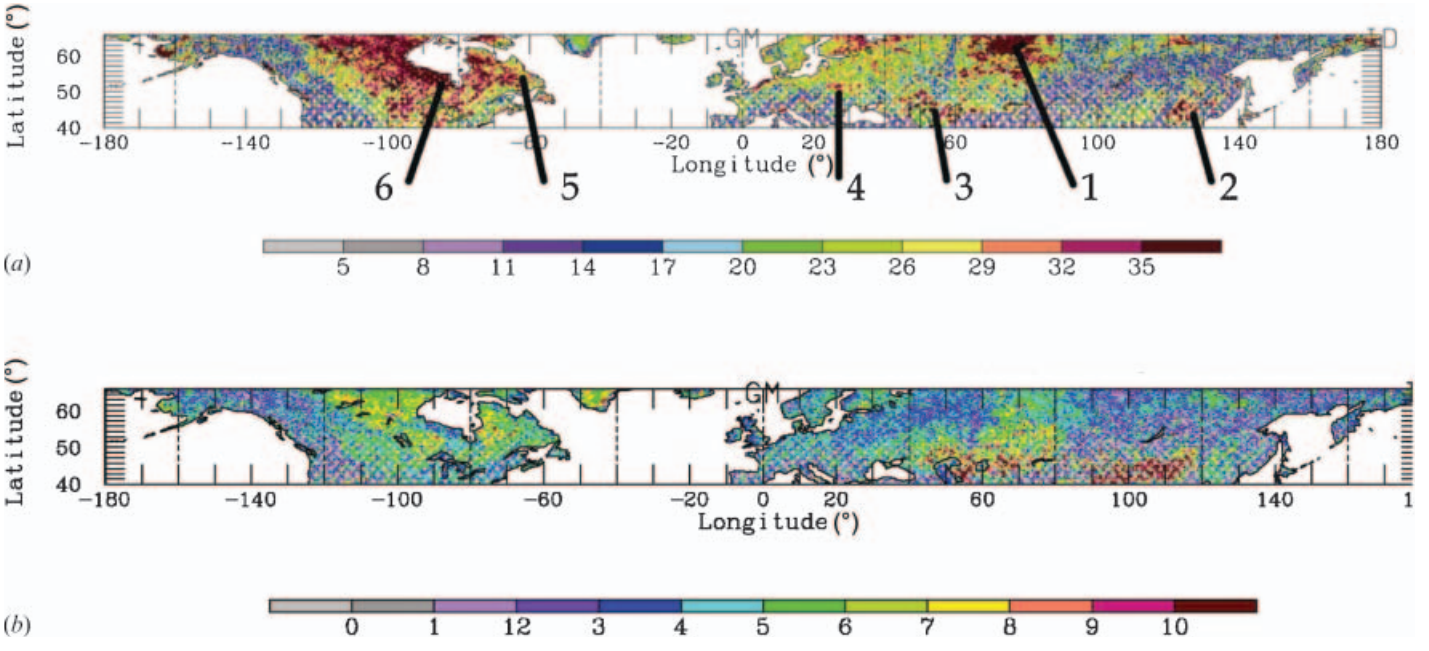

Figure 1. (*a*) Topex-Poseidon altimeter backscattering coefficient in C band and (*b*) the difference in backscatter C–Ku, expressed in dB for July 1993. The principal regions cited in the study are located in (*a*): (1) Ob River basin; (2) Amour River basin; (3) Volga River basin and the Caspian Sea; (4) Polesia region in Eastern Europe; (5) Labrador Peninsula; and (6) Hudson Bay.

by a small amount. Precipitating clouds are rare (Lin and Rossow 1997) and only affect the backscattering coefficients by about 1.5 dB at maximum (Chen *et al.* 1997, 1998).

Basically, the radar altimeter backscatter response encounters three situations over land surfaces according to their different characteristics (Ulaby *et al.* 1982, 1986).

- The land target is not composed of volumetric scatters and has no volume signal, so the return signal is only due to the surface echo, controlled by the dielectric constant and the surface roughness of the target. Because the Topex-Poseidon altimeter is nadir looking, the surface echo is not negligible and can even be the dominant term. The difference in backscatter C–Ku is low at around 2–3 dB. This response is typically the case for totally flooded areas or very dense vegetated areas with no penetration of the wave into the observed medium. For instance, in figure 1(a) and (b), we note this altimetric response for areas located around 60° N, 100° E for vegetated areas and 50° N, 90° W for totally flooded areas.
- A reflecting surface is located under volumetric scatters. The averaged signal is due to the underlying surface echo attenuated by the extinction of the radar wave within the scattering medium. The difference in backscatter C–Ku has values between 4 and 8 dB. This is typically the case for wetlands, flooded areas and soils covered by vegetation. For instance in figure 1(a) and (b), these responses are encountered over the Ob river regions (60° N, 70° E) or northern Canada. Note this is also the typical case over snow covered areas (Papa *et al.* 2002).
- The land target is a reflecting surface situated above volumetric scatters. The averaged signal is due to the surface echo and the volume echo of the underlying volume scatterers. This is the case for altimetric response encountered over major desert regions and bare soil depending on the soil moisture content. For instance in figure 1(a) and (b), this response is obtained over the Takla Makan desert (40° N, 100° E) and Central Asia (45° N, 65° E).

The last two cases, where the averaged signal depends on the volume scattering and the extinction within the medium, are frequency dependent (Remy *et al.* 1996; Papa *et al.* 2003). As a consequence, comparison of dual-frequency observations can provide additional information about the observed target. Assuming that the C–Ku signal is mainly due to the difference in the penetration of the waves in the observed target, the difference C–Ku is useful to asses the effects of vegetation (Papa *et al.* 2003).

3.2 *Comparison between microwave satellite responses*

Figure 2 displays the different individual satellite responses over a longitudinal transect crossing Europe and Asia from 50° E to 100° E at 64° N in July 1993. Large wetlands located between the Ob and Pur rivers cover the centre of the tundra region; between 68° E and 78° E, the inundation fractional cover is close to 100% (773 km^2 inundation per pixel, i.e. 100% inundation per pixel; figure 2(*f*)). A very good correspondence is obtained between the wetland spatial extent as given by Matthews and Fung (1987) and the microwave satellite responses: all microwave observations react to the presence of the standing water. Compared to bare soil and

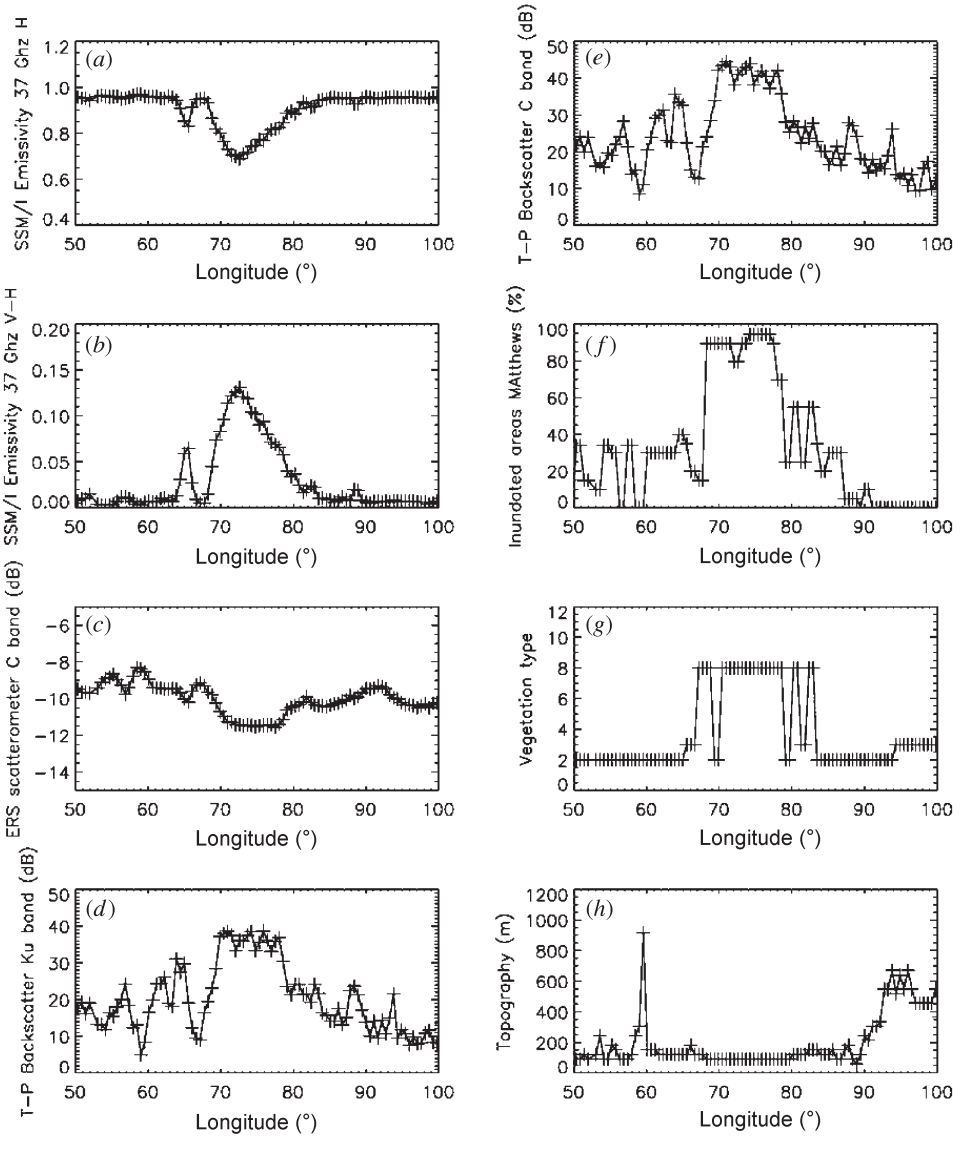

Figure 2. Longitudinal transect over Europe and Asia from 50° E to 100° E at latitude 64° N for July 1993. (*a*) SSM/I emissivity at 37 GHz horizontal polarization H; (*b*) SSM/I emissivity at 37 GHz polarization difference V–H; (*c*) ERS wind scatterometer backscatter in C band (dB); (*d*) T-P altimeter backscatter in K_u band (dB); (*e*) T-P altimeter backscatter in C band (dB); (*f*) inundated areas estimated by Matthews and Fung (1987), in % per pixel; (*g*) vegetation type (Matthews 1983), with 2=evergreen forest, 3=deciduous forest and 8=tundra; (*h*) topography from the US Navy, in meters.

vegetation, water has a high dielectric constant, which translates into microwave responses that are significantly different over open water surfaces (Ulaby *et al.* 1982). As expected, the emissivity decreases (figure 2(*a*)), which is associated with an increase of the emissivity polarization difference measured at 53° incidence (figure 2(*b*)) (Sippel *et al.* 1998, Prigent *et al.* 2001a). Over open water, the scattering coefficient is high in the specular direction: the scatterometer that measures the

radar return with a large incidence angle observes a lower backscatter (figure 2(*c*)), whereas the altimeter that performs its measurement at nadir observes strong backscattering (figure 2(*d*) and (*e*)). Within this large area between 68° E and 78° E, the altimetric responses show several smaller structures that do not appear on the scatterometer or the radiometer observations, probably because of the lower spatial resolution of these two instruments. In addition, over this open water surface, one can notice the large variation in the backscattering signal as measured by the altimeter (~30 dB between 68° E and 70° E) as compared to the scatterometer response (~3 dB in the same locations). Another noticeable structure is observable around 66° E for all satellite data. This feature also appears on the inundation information of Matthews and Fung (1987), with a maximum of 50% inundation per square degree. The altimeter response is particularly strong: it has a finer spatial resolution, and as it observes at nadir it is less attenuated by vegetation.

Outside this inundated tundra area, vegetation is dominated by forests (figure 2(*g*)), still with significant inundation extent around this central wetland. The densely vegetated areas west of 65° E (figure 2(*g*)) are characterized by high emissivities (figure 2(*a*)) with low polarization difference (figure 2(*b*)) and by rather high scatterometer backscattering (figure 2(*c*)), as expected. In these regions, detection of the standing water is more difficult with the passive instrument and with the scatterometer. For example, close to 57° E, west of the Ural Mountains, there is again a good agreement between the altimeter response and the inundation information but the corresponding signatures with the scatterometer and the radiometer are weaker.

In this transect, it is clear that the altimeter backscattering strongly responds to the presence of inundation, with a good sensitivity and better spatial resolution as compared to the other microwave instruments, even in forested regions.

For a closer examination of the relation between the altimeter and the passive microwave observations, scatter plots of the altimetric measurements versus the other microwave information are presented over the inundated Ob River plain located in northern part of Russia (62–66° N and 68–72° E) for July 1993 (figure 3).

The passive microwave and altimetric responses in both bands are strongly correlated, with linear correlation coefficient of ~0.8, despite the differences in observation frequencies (5 GHz and 13.6 GHz versus 37 GHz shown on the graph; we checked that similar correlation coefficients are obtained for the other SSM/I frequencies), in incidence angle (nadir compared to 53°), and in spatial resolution. With increasing altimetric backscattering, the emissivity declines and the emissivity polarization difference increases. The saturation effect observed with the altimeter at high backscattering coefficient is likely due to the spatial resolution difference between the two instruments: open water can completely fill the altimeter field-of-view (FOV) when it still only partially covers the radiometer FOV. Although using the same frequency at C band, the scatterometer and the altimeter signals are not well correlated. Unexpected relations between the radiometer and the scatterometer responses have already been noted (Prigent *et al.* 2001a, b) and over the Ob region correlation coefficients are also low (~0.45). The scatterometer at 5 GHz is surprisingly less sensitive to standing water than the radiometer at 19 or 37 GHz over vegetated areas, although their incidence observation angles and spatial resolutions are similar. Because of the longer wavelength of the scatterometer, more penetration in the vegetation was expected, and as a consequence more sensitivity to standing water below the canopy. More comparison studies and modelling efforts are needed for a better understanding of the scatterometer response.

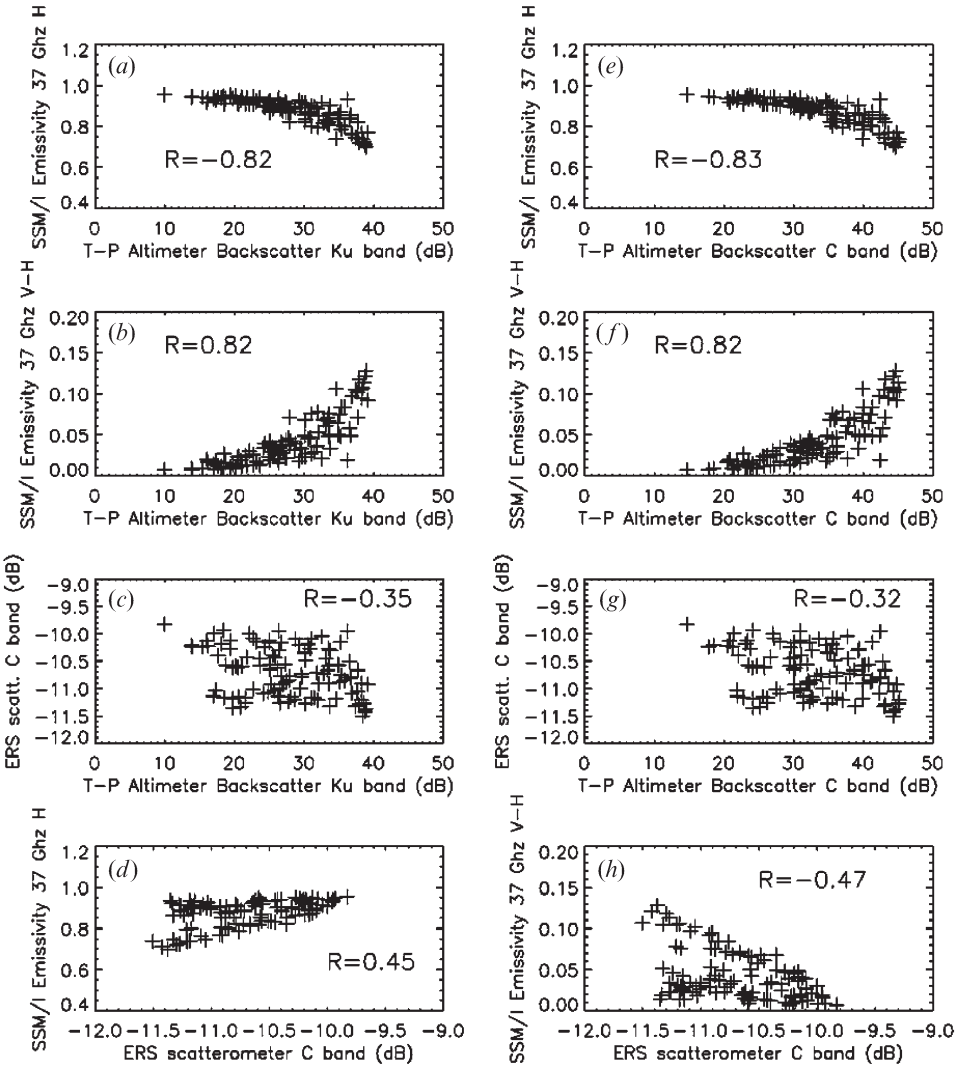

Figure 3. Active and passive microwave responses over the Ob River plain, Russia for July 1993. Topex-Poseidon backscatter in Ku band versus SSM/I emissivity at 37 GHz in vertical polarization V (*a*), the difference V–H (*b*) and the ERS wind scatterometer backscatter in C band (*c*). Topex-Poseidon backscatter in C band versus SSM/I emissivity at 37 GHz in vertical polarization V (*e*), the difference V–H (*f*) and the ERS wind scatterometer backscatter in C band (*g*). ERS wind scatterometer backscatter in C band versus SSM/I emissivity at 37 GHz in vertical polarization V (*d*) and the difference V–H (*h*).

These comparisons between the satellite microwave observations show that the altimeter backscattering is very sensitive to the presence of standing water, with a better spatial resolution and less sensitivity to the vegetation than the other microwave observations. In inundated regions, it is very well correlated with the passive microwave observations that have already been used for wetland detection (Sippel *et al.* 1998, Prigent *et al.* 2001a). We thus suggest the development of a method to estimate the wetland extent from the altimetric backscattering over boreal regions.

4. Estimation of wetland extent and seasonality using the altimeter and analysis of the results over the Northern Hemisphere

4.1 *Methodology*

The proposed methodology is based on the detection of inundated areas using the altimetric backscattering coefficient in C band. C band was chosen because the altimeter signal at this frequency is less sensitive to the presence of the vegetation than the Ku band (Papa *et al.* 2003). In a first step, a threshold on the altimetric signal in C band is used to define whether or not a pixel is inundated. In a second step, the inundation fraction of the observed pixel is calculated using the C backscatter magnitude. Finally, the vegetation contribution is taken into account using the C–Ku signal difference.

The first step of this methodology is to detect an inundated pixel using a threshold in the C altimetric signal. According to figure 2 (*a*, *b*, *e* and *f*) and figure 3 (*e* and *f*) related to the Ob region study, a C backscattering value of 20 dB or larger is consistent with the presence of water as derived from the climatology of Matthews (2000) or by comparison with other satellite data. This value of the threshold in C band is also consistent with the study of Birkett (2000), where T-P Ku band backscatter values higher than 17 dB were used to detect water surface over the Lake Chad region. With an intrinsic difference between C and Ku band altimetric backscatters of ~3 dB over ocean (Chapron *et al.* 1995), the 17 dB threshold from Birkett (2000) in Ku band translates into a 20 dB threshold in C band. The study of other inundated regions by the authors, such as over Canada (not shown) confirms the threshold of 20 dB in C band.

Once an area is determined to be inundated, the inundation fraction of the observed pixel is then estimated, assuming that the surface extent of the observed pixel is proportional to and varies linearly with the backscatter in C band: using a linear mixing model, the inundation fraction increases by 4% when C band backscatter increases by 1 dB. A pixel starts to be inundated when the backscatter in C band has a value greater than 20 dB and 100% inundation for the pixel corresponds to 45 dB, as can be observed from figure 2. Examination of other inundated regions, over Canada for instance, confirmed this relation.

Finally, the response to inundation of C band backscatter can be modulated by vegetation and this contribution needs to be taken into account. Assuming that C–Ku is mainly due to the difference in the penetration of the waves to the observed target (Remy *et al.* 1996), the value of C–Ku can be related to the presence of overlying vegetation (Papa *et al.* 2003). The inundation fraction previously calculated decreases with increasing backscattering difference C–Ku, related to the difference of penetration into the vegetation. The fractional extent of inundated areas decreases by 4% for each 1 dB increase of C–Ku.

This method is used to calculate the monthly mean flooded fraction for the region located between 40° N and 66° N from January 1993 to December 1994. Note that during the wintertime, the altimetric backscattering coefficients in Ku and C bands are sensitive to the snow: they decrease at the beginning of the snow season and are related to the snow depth evolution (Papa *et al.* 2002). Their values are usually less than 20 dB during the winter period, so confusion with inundated pixels is unlikely. However, frozen lakes and rivers or melting snow can exhibit a high altimetric backscattering signal and to avoid any ambiguity with inundated pixels, the snow and ice mask from the NSIDC has been used to edit the results.

4.2 *Spatial and temporal dynamics of the wetlands*

The results using the radar altimeter focus on the large-scale distribution of the inundated areas, their seasonality, and their duration. Since it is not possible with the present method to distinguish between natural wetlands and lakes or rivers, the results will be compared with independent datasets that together capture the full range of inundation.

4.2.1 Wetland extent. Figure 4 shows the fractional extent of wetlands obtained with Topex-Poseidon altimeter for July 1993. Other independent datasets of global wetland distributions are presented in figure 5: the estimate from Cogley (1991) (figure 5(*b*)) and from Matthews and Fung (1987) (figure 5(*c*)), along with the lakes distribution from Cogley (1991) (figure 5(*a*)). The Cogley (1991) and Matthews and Fung (1987) estimates do not have seasonal variations but are likely representatives of the warm season with maximum flooding. Given the lack of validation sources at global scales, these independent datasets help qualitatively to evaluate our results.

As compared to the other estimates, the new results in figure 4 exhibit realistic structures. The inundated region around the Ob River in northern Russia is well reproduced and agrees well with the estimates of Cogley (1991) and Matthews and Fung (1987). Wetlands located in northern Russia between 25° E and 35° E and above 60° N are reproduced with fractional values ranging between the ones proposed by Cogley (1991) and Matthews and Fung (1987). The inundated region around the Amour River in the far eastern part of Russia (~45° N and 125° E) is also correctly detected. These results also demonstrate that the radar altimeter can detect small wetlands like the inundated regions located at 58° N and 28° E in Belarus (Polesia) that also appears on the Cogley map. However, north of the Caspian Sea, the radar altimeter technique detects large wetlands that are not reported on the other estimates. Because of the lack of other independent *in situ* datasets in that region, we cannot conclude if this result is an overestimation due to our method or if this region of the Volga River was really inundated during this period.

Over North America, extensive features are also realistically represented. The large wetlands close to the Hudson Bay are clearly captured and are in accordance with Cogley (1991): note that in this region, there is also a large distribution of small lakes that significantly contribute to the altimetric signal. Above 60° N, the radar altimeter technique detects large structures with realistic spatial distribution but the inundated fractions are higher than the ones estimated by Cogley (1991). This is also the case for the Labrador Peninsula, in eastern Canada. However, strong inundated fractions over these areas were also observed in Prigent *et al.* (2001a) using other microwave satellite observations. The complex structures of these areas, with small lakes, large pools and inundated tundra, might partly explain the discrepancies between the maps derived from the examination of airborne pictures and satellite estimates.

4.2.2 ***Seasonality and duration.*** Figure 6 shows the number of inundated months for each pixel between January 1994 and December 1994. For each month, only the pixels with fractional extent of water above 10% are included. The radar altimeter shows realistic inundation durations for the Boreal region. The method detects flooding for 4–6 months south of the Ob River declining to 2–3 months for the northern area. Duration of flooding is also around 3–4 months for north-eastern part of Russia. Over northern America, inundation duration ranges from 4–5

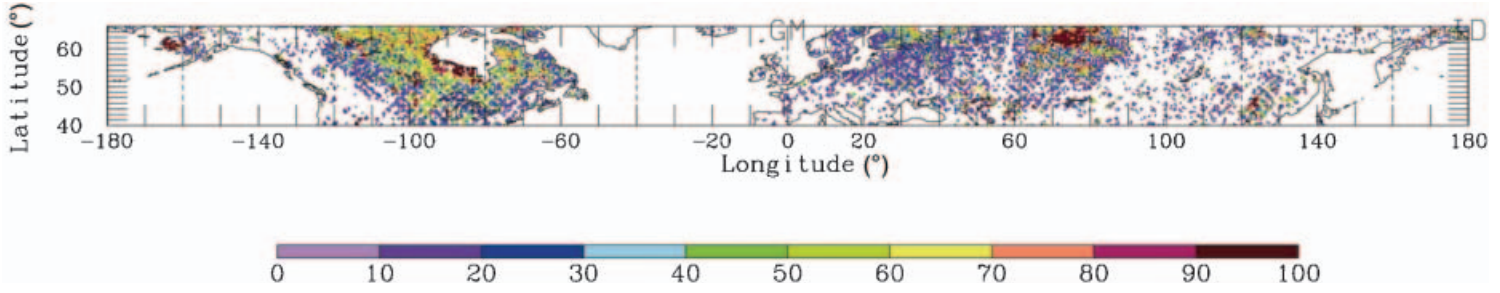

Figure 4. Estimation with Topex-Poseidon radar altimeter of fractional extent of wetlands for July 1993 over the Northern hemisphere from 40° N to 66° N.

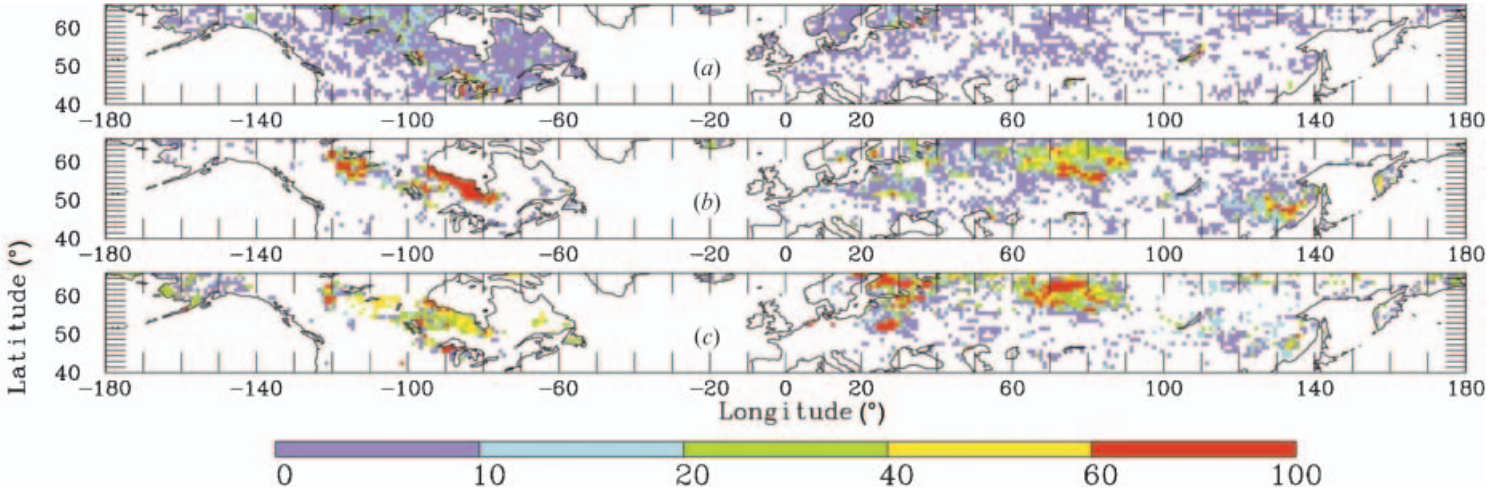

Figure 5. (*a*) Fractional extent of lakes (Cogley 1991); (*b*) fractional extent of wetlands (Cogley 1991); (*c*) fractional extent of natural wetlands (Matthews *et al.* 1987).

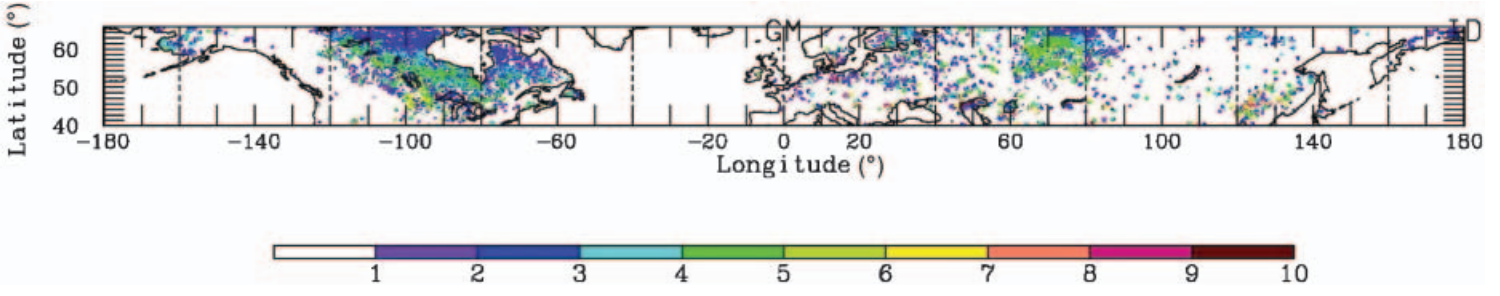

Figure 6. Number of inundated months for each pixel between January 1994 and December 1994 estimated with Topex-Poseidon radar altimeter.

months south of 55° N to 2–3 months for northern locations. These results are consistent with previous results from Walter and Heinmann (2000) and from satellite-derived estimates from Prigent *et al.* (2001a).

Little information is available about the seasonal variations of wetlands and there are almost no datasets describing the wetlands dynamics at regional scales for a year or longer. Figure 7 displays the seasonal variations of the total wetland extent for the boreal region between 55° N and 66° N from January 1993 to December 1994 with the T-P radar altimeter technique and with the satellite-derived method from Prigent *et al*. (2001a). The new results show a seasonal variation with a maximum reached during the warm season for both years, similar to results obtained by Prigent *et al.* (2001a) for the same period. However, the maximum extents are different, with $1.86 \times 10^6\,\mathrm{km}^2$ derived from the altimeter data and $1.31 \times 10^6\,\mathrm{km}^2$ from the other technique. Matthews and Fung (1987) give a wetland extent of $2.12 \times 10^6\,\mathrm{km}^2$ whereas Cogley (1991) estimates $1.47 \times 10^6\,\mathrm{km}^2$ for the wetlands and $2.08 \times 10^6\,\mathrm{km}^2$ for the wetlands plus the lakes.

Over all the northern wetlands, the altimeter-derived extent is within 10% of the estimates from the completely independent datasets from Cogley and Matthews. This result is very encouraging, given the large intrinsic uncertainties on each of these climatological estimates. It represents though a first step in describing the wetland variations at a regional or global scale. Moreover, considering the entire northern wetlands estimations, these results are in agreement with the technique from Prigent *et al.* (2001a), although the latter does give a lower estimate. This could be explained by (1) the spatial resolution of the instruments, which makes the estimate less sensitive to the presence of small lakes and wetlands that are very common in these boreal regions, and (2) higher sensitivity to the vegetation due to the use of higher frequencies and larger scanning angles.

Finally, over a specific region such as the Ob River basin, the new results with the radar altimeter show seasonal variation, with maxima reached during the summer

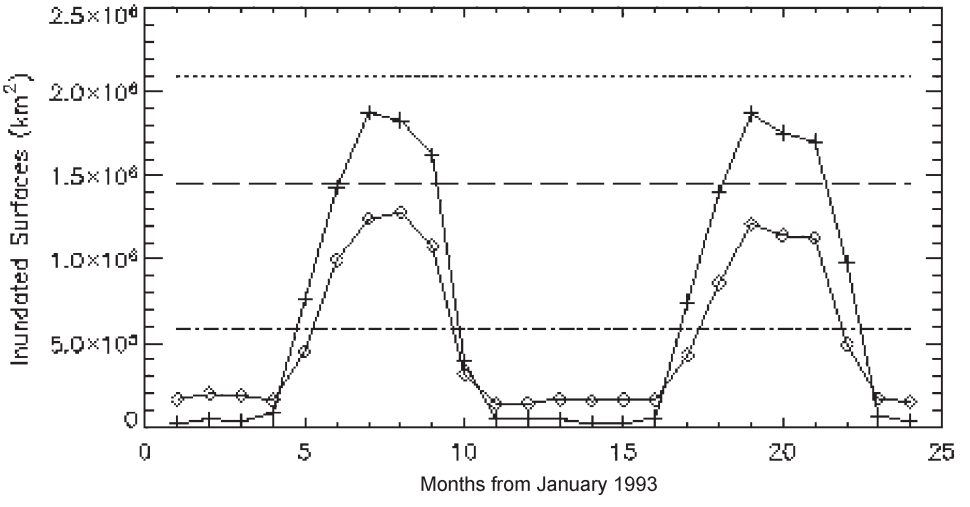

Figure 7. Seasonal variations of inundated areas over the boreal regions from 55° N to 66° N for each month between January 1993 and December 1994 with the Topex-Poseidon radar altimeter (+) and with the satellite-derived method from Prigent *et al*. (2001a) (◇). The wetland extents from Cogley (1991) (— —) and Matthews and Fung (1987) (- - -) are added, along with the surface of the perennial lakes from Cogley (1991) (– - – -).

season for both years (1993 and 1994), which are close to the estimates obtained by Prigent *et al.* (2001a) (figure 8(*a*)). However, the technique of Prigent *et al.* (2001a) again gives a lower estimate at the end of the summer. Comparison of the altimeter-derived extent with independent dataset from Matthews and Fung (1987) shows a difference within 15% (figure 8*a*).

Moreover, the seasonality of the inundation extent around rivers can be evaluated by comparison with river level measurements obtained with the T-P radar altimeter: similar temporal variability should be observed. The monthly mean levels of the Ob River derived from the radar altimeter are shown for 1993–1994 in figure 8(*b*) (Kouraev *et al.* 2004). These results show good agreement with coincident maxima and minima, and variations of wetland extent over the Ob river plain, providing confidence in the technique.

5. Conclusion and perspective

The present study reports on a new effort to quantify the extent and seasonality of wetlands using satellite altimeter observations over boreal regions. First, the

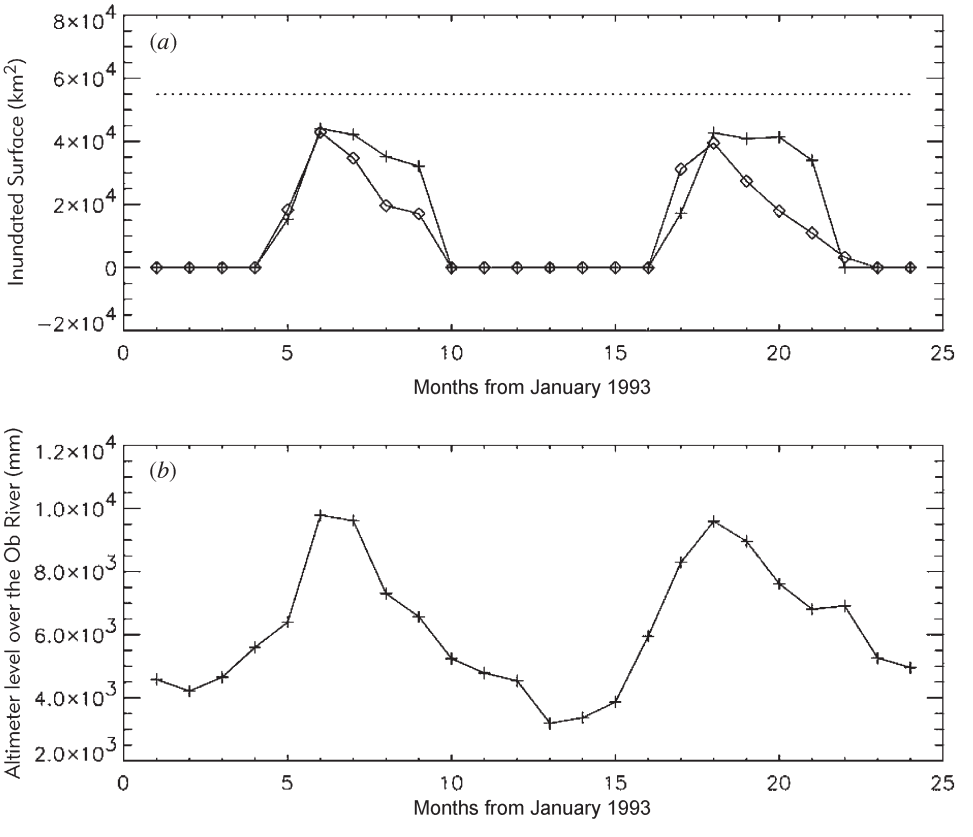

Figure 8. (*a*) Seasonal variations of inundated areas (km^2) over the Ob River basin between January 1993 and December 1994 with the Topex-Poseidon radar altimeter (+), and with the remote sensing technique from Prigent *et al.* (2001) (◇). The wetland extents from Matthews and Fung (1987) (- - -) are added. (*b*) Monthly average level (mm) for the Ob River derived from Topex-Poseidon radar altimeter measurements for each month between January 1993 and December 1994.

altimeter response is compared with other satellite microwave observations that have already been used for wetland estimations. We conclude that the altimeter is very sensitive to the presence of water, with a higher spatial resolution than other microwave measurements and less contamination by vegetation. A method is developed to estimate the wetland extents over the boreal regions where the Topex-Poseidon altimeter spatial coverage is satisfactory. The results from the whole boreal region for the 1993 and 1994 periods show spatial structures and seasonal dynamics that are in good agreement with existing estimates from remote sensing techniques or independent climatological datasets. For the Ob wetlands, the seasonal variability of the inundation extent and river gage levels have also been compared. The various comparisons with independent data showed very encouraging agreements, providing some confidence in the estimation technique. Further validation of the products is hampered by the lack of other global scale wetland estimates.

The application of this methodology to the 10-year span dataset (1992–2003) of Topex-Poseidon is planned, as well as the use of the new measurements from the dual-frequency altimeter on board Jason-1. These promising results also need to be checked with the use of the ENVISAT dual-frequency radar altimeter dataset processed by the ICE-2 algorithm, which is devoted to continental studies (Legresy *et al.* 2005). The ENVISAT dataset offers all waveform parameters such as backscatter, leading edge width, trailing edge slope and range over lands in S and Ku band (Legresy *et al.* 2005). The surface/volume signal obtained from these parameters will certainly help better detect the inundated surfaces. Moreover ENVISAT, with its polar orbit and its 35-day repeat cycle, has a dense spatial coverage (inter-track at the equator of 80 km) and will allow a survey of the world's inundated surfaces (Legresy *et al.* 2005). With more investigation, the developed technique, using Topex-Poseidon over the northern wetlands or using Envisat on a global scale, may be applicable without any tuning for other environments, such as the tropics.

Finally, future studies will explore the possibility of using the estimated inundation extents and the water levels also derived from the altimeter to evaluate the variations of the volumes of water stored in the main river corridors, interior wetlands and flooded forests that are a key for hydrological studies.

Acknowledgments

The authors thank the CTO (Centre de Topographie des Oceans) at the LEGOS (Laboratoire d'Etudes en Géophysique et Océanographie Spatiales, CNES, Toulouse) for providing them with the Topex-Poseidon radar altimeter data. The authors thank A. Kouraev from the LEGOS for Ob River levels from Topex-Poseidon. The data can be provided upon request to one of the authors. The ERS-1 wind-scatterometer data have been provided by the European Space Agency (ESA).

References

Allison, R.G.B. and Goodison, B., 2001, CLIC, Climate and Cryosphere Project. Science and Co-ordination plan. WRCP-114, WMO/TD.

Alsdorf, D., Birkett, C.M., Dunne, T., Melack, J. and Hess, L., 2001, Water level change in large Amazon lake measured with space born radar interferometry and altimetry. *Geophysical Research Letters*, **28**, pp. 2671–2674.

Birkett, C.M., 1995, The contribution of TOPEX/POSEIDON to the global monitoring of climatically sensitive lakes. *Journal of Geophysical Research*, **100**, pp. 25 179–25 204.

BIRKETT, C.M., 1998, The contribution of the TOPEX (NRA) radar altimeter to the global monitoring of large rivers and wetlands. *Water Resources Research*, **34**, pp. 1223–1240.

BIRKETT, C.M., 2000, Synergetic remote sensing of Lake Chad: variability of basin inundation. *Remote Sensing of Environment*, **72**, pp. 218–236.

CAZENAVE, A., BONNEFOND, P. and DOMINH, K., 1997, Caspian Sea level from Topex-Poseidon altimetry: level now falling. *Geophysical Research Letters*, **24**, pp. 881–884.

CHAPRON, B., KATSAROS, K., ELFOUHAILY, T. and VANDERMARK, D., 1995, A note on relationships between sea surface roughness and altimeter backscatter. In *3rd International Symposium on Air–Water Gas Transfer* (Heidelberg, Germany: Heidelberg University), 24–27 July 1995, pp. 869–878.

CHEN, G., CHAPRON, B., TOURNADRE, J., KATSAROS, K. and VANDEMARK, D., 1997, Global oceanic precipitation: a joint view by TOPEX and the TOPEX microwave radiometer. *Journal of Geophysical Research*, **102**, pp. 10 457–10 471.

CHEN, G., CHAPRON, B., TOURNADRE, J., KATSAROS, K. and VANDEMARK, D., 1998, Identification of possible wave damping by rain using TOPEX and TMR data. *Remote Sensing of Environment*, **63**, pp. 40–48.

COGLEY, J.G., 1991, GGHYDRO-Global Hydrographic data release 2.0. Trent Climate Note 91-1, Trent University, 12.

DICKINSON, B.I., YASHAYAEV, J., MEINCKE, B., TURRELL, S.D. and HOLFORT, J., 2001, Rapid freshening of the deep north Atlantic Ocean over the past four decades. *Nature*, **416**, pp. 832–837.

FRISON, P.L. and MOUGIN, E., 1996a, Use of the ERS-1 wind scatterometer data over land surfaces. *IEEE Transactions on Geoscience and Remote Sensing*, **34**, pp. 550–560.

FRISON, P.L. and MOUGIN, E., 1996b, Monitoring global vegetation dynamics with the ERS-1 wind scatterometer data. *International Journal of Remote Sensing*, **17**, pp. 3201–3218.

FUNG, L.L. and CAZENAVE, A., 2001, Satellite altimetry and earth science. In *A Handbook of Techniques and Applications*, International Geophysical Series, 69 (San Diego: Academic Press).

HOLLINGER, J.P., PIERCE, J.L. and POE, G.A., 1990, SSM/I instrument evaluation. *IEEE Transactions on Geoscience and Remote Sensing*, **28**, pp. 781–790.

JUSTICE, C.O., TOWNSHEND, J.R.G. and CHOUDHURY, B.J., 1989, Comparison of AVHRR an SMMR data for monitoring vegetation phenology on a continent scale. *International Journal of Remote Sensing*, **10**, pp. 1607–1632.

KOURAEV, A., PAPA, F., BUHARIZIN, P.I., CAZENAVE, A., CRETAUX, J.F., DOZORSTEVA, J. and REMY, F., 2003, Ice cover variability in the Caspian and the Aral seas from active and passive satellite microwave data. *Polar Research*, **22**, pp. 43–50.

KOURAEV, A., ZAKHAROVA, E., SAMAIN, O., MOGNARD-CAMPBELL, N. and CAZENAVE, A., 2004, Ob river discharge from Topex/Poseidon satellite altimetry data. *Remote Sensing of Environment*, **93**, pp. 238–245.

LEGRESY, B. and REMY, F., 1997, Altimetric observations of surface characteristics of the Antarctic ice sheet. *Journal of Glaciology*, **43**, pp. 265–275.

LEGRESY, B., PAPA, F., REMY, F., VINAY, G., VAN DEN BOSCH M. and ZANIFE, O.Z., 2005, ENVISAT radar altimeter measurements over continents and ice caps using the Ice-2 retracking algorithm. *Remote Sensing of Environment*, **95**, pp. 150–163.

LIN, B. and ROSSOW, B.W., 1997, Precipitation water path and rainfall rates estimates over oceans using Special Sensor Microwave Imager and International Satellite Cloud Climatology Project data. *Journal of Geophysical Research*, **102**, pp. 9359–9374.

MATTHEWS, E., 1983, Global vegetation and land use: New high-resolution data bases for climate studies. *Journal of Climate and Applied Meteorology*, **22**, pp. 474–486.

MATTHEWS, E., 2000, Wetlands. In *Atmospheric Methane: its role in the global environment*, M..A.K. Khalil (Ed.), pp. 202–233 (Berlin: Springer Verlag).

MATTHEWS, E. and FUNG, I., 1987, Methane emission from natural wetlands: global distribution areas and environmental characterization of sources. *Global Biogeochemical Cycles*, **1**, pp. 61–86.

PAPA, F., LEGRESY, B., MOGNARD, N.M., JOSBERGER, E.G. and REMY, F., 2002, Estimating terrestrial snow depth with the Topex-Poseidon altimeter and radiometer. *IEEE Transactions on Geoscience and Remote Sensing*, **40**, pp. 2162–2169.

PAPA, F., LEGRESY, B. and REMY, F., 2003, Use of the Topex-Poseidon dual-frequency radar altimeter over land surfaces. *Remote Sensing of Environment*, **40**, pp. 2162–2169.

PRIGENT, C., ROSSOW, W.B. and MATTHEWS, E., 1997, Microwave land surface emissivities estimated from SSM/I observations. *Journal of Geophysical Research*, **102**, pp. 21 867–21 890.

PRIGENT, C., MATTHEWS, E., AIRES, F. and ROSSOW, W., 2001a, Remote sensing of global wetlands dynamics with multiple satellite data sets. *Geophysical Research Letters*, **28**, pp. 4631–4634.

PRIGENT, C., AIRES, F., ROSSOW, W. and MATTHEWS, E., 2001b, Joint characterisation of vegetation by satellite observations from visible to microwave wavelengths: a sensitivity analysis. *Journal of Geophysical Research*, **106**, pp. 20 665–20 685.

REMY, F., LEGRESY, B., BLEUZEN, S., VINCENT, P. and MINSTER, J.F., 1996, Dual frequency Topex altimeter observations of Greenland. *Journal of Electromagnetic Waves and Applications*, **10**, pp. 1507–1525.

REMY, F., SCHAEFFER, P. and LEGRESY, B., 1999, Ice flow physical processes derived from ERS-1 high resolution map of the Antarctica and the Greenland ice sheets. *Geophysical Journal International*, **139**, pp. 645–649.

RODRIGUEZ, E. and MARTIN, J.M., 1994, Assessment of the Topex-Poseidon altimeter performance using waveform retracking. *Journal of Geophysical Research*, **99**, pp. 24 977–24 980.

SIPPEL, S.J., HAMILTON, S.K., MELACK, J.M. and NOVE, E.M., 1998, Passive microwave observations of inundated area and area/stage relation in Amazon River floodplains. *International Journal of Remote Sensing*, **19**, pp. 3055–3074.

ULABY, F.T., MOORE, R.K. and FUNG, A.K., 1982, *Microwave Remote Sensing: Active and Passive, Volume II: Radar Remote Sensing and Surface Scattering and Emission* (Norwood, MA: Addison-Wesley).

ULABY, F.T., MOORE, R.K. and FUNG, A.K., 1986, *Microwave Remote Sensing: Active and Passive, Volume III: From Theory to Applications* (Norwood, MA: Addison-Wesley).

WALTER, B., HEINMANN, M. and MATTHEWS, E., 2001, Modeling modern methane emission from natural wetlands, model description and results. *Journal of Geophysical Research*, **106**, pp. 34189–34206.

ZIEGER, A.R., HANCOCK, D.W., HAYNE, G.S. and PURDY, G.L., 1991, NASA radar altimeter for the Topex-Poseidon project. *IEEE Transactions on Geoscience and Remote Sensing*, **79**, pp. 810–826.

ZWALLY, H.J., BINDSCHADER, R.A., BRENNER, A.C., MARTIN, T.V. and THOMAS, R.H., 1983, Surface elevation contours of Greenland and Antarctica ice sheets. *Journal of Geophysical Research*, **88**, pp. 1589–1596.